MODERN DESIGN OF AUTOMOTIVE AXIAL COOLING FANS USING INVERSE METHODS

Mihai BLEIZIFFER[1], Anand SIVARAMAKRISHNAN[1],
Rainer SCHOELE[1], Mehrdad ZANGANEH[2], Jiangnan ZHANG[3]

[1] *Hanon Systems EFP Germany, eCF Group, Bad Homburg, Germany*

[2] *Department of Mechanical Engineering, University College London, UK*

[3] *Advanced Design Technology Ltd, London, UK*

SUMMARY

This paper shows briefly the advance in the aerodynamic and acoustic development for a new axial electronic cooling fan family by using inverse design. This is realized by using reverse engineering function of inverse design method to obtain blade loading of existing optimized designs and then use this loading incorporating features used in current existing serial designs.

INTRODUCTION

Hanon Systems provides complete solutions for automotive cooling systems including electronic cooling fans (eCF's) for power classes starting from 300W and reaching up to 1.5 kW. This paper focuses on the development of electronic cooling fans in the "high power" class.

We present a methodology in which the important know-how of an optimum existing design is captured by using an inverse design method to reverse engineer the existing blade and hence recover the optimum loading of the fan blade. Then use this optimum loading as a basis for the design optimization of the automotive cooling fan that meets the new challenging requirements. In this paper, we want to show how this approach was implemented as well as the benefits gained on performance, acoustics and time-to-delivery.

In order to combine both existing methods, a complex aerodynamic design process involving reverse engineering, CFD simulations and experimental validation has been set up. Starting from the loading obtained from reverse engineering of an existing design, a process was followed in which the spanwise work and streamwise loading were varied systematically by using the inverse design method and the resulting performance evaluated by using a previously validated CFD simulation set up. Parallel, structural and modal analysis simulations were performed to ensure the structural integrity of the design during operation. Performance measurements have confirmed the CFD simulations results and acoustic measurements showed an excellent behavior.

AERODYNAMIC DESIGN

Aerodynamic design process

The inverse aerodynamic design process of axial fans is described in the literature in several papers of Bleiziffer, Smith and Semel [6,7,8]. The author shows in [6] that total-to-static pressure and efficiency are the correct design parameters when designing an axial fan while Epple [9] shows how this performs theoretically in terms of ideal total-to-static efficiency and refers to the Cordier Diagram. The design process is presented in detail in the works of the author [6,7] and by Semel [10] in which designing and improving axial fans geometry is done by using inverse design methods.

At Hanon Systems the aerodynamic process cycle is streamlined by using either validated in-house or commercial available software tools (see Figure 1). The processes involved in the fan aerodynamic development will be presented in the next sections.

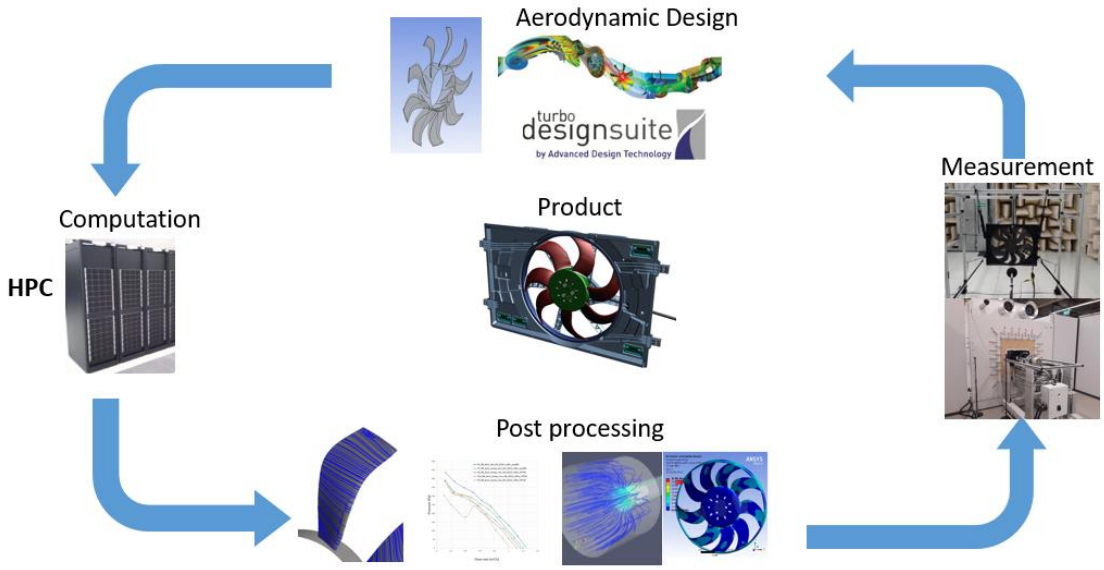

Figure 1: Typical development process of a fan at Hanon Systems in Bad Homburg

Aerodynamic design targets

Fixing the aerodynamic design targets for a new development is one of the most important and challenging processes within the fan development. This is very complex because all requirements of the product come together: airflow and pressure (aerodynamics), NVH, power and torque capabilities of the electric drive and structural integrity during operation. These are constraining requirements and as one of them gets improved most of the others deteriorate and the challenge is to find the optimum balance between them. One of the most important requirements is the dimension of the fan, which is decided based on the packaging constraints as well as on the heat exchanger used. Fan load points are calculated based on the provided air flow losses of the heat exchanger.

A 1D matching process is used to match a fan to the (customer) requirements. In this process the curves of all tested portfolio blades are scaled and the best matching is found to the desired targets. However, due to physical limitations related to size, shape, structure and drive performances it is not always possible to use previously designed blades. In this case a new fan blade shape has to be designed to achieve the load points.

Background of inverse 3D blade design method

The 3D inverse design method first introduced in [1], has been used extensively in design of all types of fans including axial fans [2] and centrifugal blowers [3]. The 3D inviscid code computes the blade geometry subject to specified blade loading on the surface. The circumferentially averaged bound circulation is used as input to specify the blade loading. It is defined as:

$$r\overline{V_\theta} = \frac{N}{2\pi}\int_0^{2\pi/N} r \cdot V_\theta d\theta \qquad (1)$$

The Euler head (work coefficient) can be fixed by specifying the spanwise $r\overline{V_\theta}$ distribution at the leading edge and trailing edge of the blade. The spanwise $r\overline{V_\theta}$ can be constant from hub to tip (so called free vortex design) or it can vary arbitrarily. Previous work has shown that for axial fans the parabolic spanwise $r\overline{V_\theta}$ distribution can result in improvements in efficiency and noise, see [4].

For incompressible flow the meridional derivative of $r\overline{V_\theta}$ is related to the pressure difference between the blade pressure surface and suction surface:

$$p^+ - p^- = \frac{2\pi}{N}\rho W_{mbl}\frac{\partial(r\overline{V_\theta})}{\partial m} \qquad (2)$$

By prescribing the meridional derivative $\partial(r\overline{V_\theta})/\partial m$ (blade loading) in the blade passage the corresponding blade geometry can be computed by the inverse design procedure. Therefore, the blade geometry is controlled by the aerodynamic inputs which are related to the flow behavior. Figure 2 shows the blade loading parameters required in the commercial version of the inverse design method TURBOdesign1 [19] to control the blade geometry. $r\overline{V_\theta}$ is normalized by the impeller outlet tip radius and speed in TURBOdesign1. The normalized value ($r\bar{V}_\theta^*$) is used in specifying the loading. Three segments (two parabolic curves and a linear line connecting the two) are used on the hub and shroud streamlines. Four parameters (NC, ND, SLOPE and DRVTLE) are needed to define a loading curve.

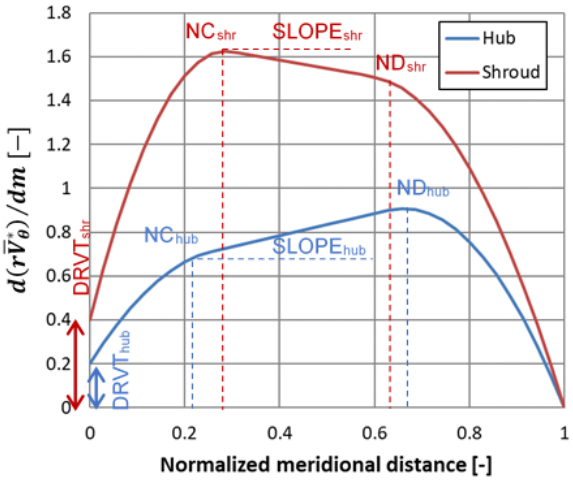

Figure 2: The blade loading parameters used in inverse design method

The value of DRVTLE ($\partial(r\overline{V_\theta})/\partial m$ at the leading edge) affects the blade incidence and the peak efficiency point of the design.

Therefore only 8 parameters are needed to define a complex 3D blade shape, which greatly reduces the degree of freedom in optimization process compared to a direct design approach, see [5]. Furthermore, each design generated by inverse design method will satisfy the specified Euler head through the specified spanwise $r\overline{V_\theta}$. In addition, the stacking condition can be specified at a chordwise location between the blade leading edge and trailing edge. The stacking condition is used as an initial condition in the inverse design process to compute the blade shape. It is introduced by specifying variation of wrap angle from hub to tip at one quasi-orthogonal location.

This can introduce an additional means of controlling the spanwise pressure field in the rotor. In axial fans the stacking is also used to control the backward or forward sweep of the rotor.

One of the key features of using 3D inverse design method is the fact that blade loading has generality, especially since the inverse design method uses the normalized loading with swirl velocity normalized by the tip speed or ($r\bar{V}_\theta^*$). So for example the type of blade loading that

maximizes efficiency of an axial fan say for automotive cooling with special geometry of the shroud ring can be used for fans of similar application perhaps with higher or lower diameters or flow rates. This generality of blade loading could be used as a powerful means of translating database of optimized fan geometries to useful know-how that can be used quickly to optimize new designs. Something that is not so easily possible with conventional design as changes to diameter will impact the blade angle distributions etc. This feature of inverse design was used for this study by first finding the blade loading of an existing design with slightly different specification to the fan being developed.

Capturing design features from current designs

An existing fan having 86 % of the diameter of the target fan has been chosen as a baseline for the new development. Acoustics and performance lines of the fan are known, in this case is the same fan that was used as CFD baseline (see the subsection correlation to test-rig). However, if this fan would have been scaled to the needed dimension, the load on the drive (torque) would have exceeded its specification. To better match the system a new fan blade with customized aerodynamics and improved aeroacoustics was developed for the new High Power drive generation from Hanon Systems.

The inverse design method needs following input for the design of an axial fan:

- design point: flow-rate, density, static pressure, rpm
- radial load distribution (spanwise distribution)/derived from t-t or t-s pressure
- streamwise load distribution (usually specified at hub, -mid and tip section)
- meridional geometry
- thickness distribution (at least at hub and at tip)
- radial sweep distribution specified by the stacking condition

Last 3 represent geometric inputs which are needed so a design is generated. Meridional section combined with the meridional load distribution is responsible for the chord length and the chord length distribution which are more usual input for inverse design of axial fans or propellers (see i.e. Bleiziffer [11]). However, in these publications the incidence angle (which for a radial section is the angle-of-attack/AoA) at the design flow-rate is also given as an input (for example for NACA meanlines as the ideal AoA [12]) while in TURBOdesign1 the 3D blade shape is computed for a given prescribed loading distribution and the incidence or angle-of-attack is set by the choice prescribed loading. The result can always be seen by checking the meridional angle distribution as well as the calculated airfoil load. The procedure of capturing the original design parameters has been performed in the virtual environment on two different levels: one was the pure geometric re-parametrization using TURBOdesign1 is reverse engineering capabilities and the other was capturing the performance data (blade loading) from CFD simulation. The results from TURBOdesign1's reverse engineering functionality are depicted in Figure 3.

First, the original geometry has been prepared for simulation in Ansys Design Modeler (using the turbo mode) where the blade geometry is basically cut in its fundamental pieces: hub- and shroud curves plus the airfoils in between. These can be used to retrieve the mri and thickness of the blade as well as can be used to visualize blade angles at the respective sections using TURBOdesign CAD. During the process all three geometric design characteristics mentioned above have been retrieved. The spanwise work distribution was captured from the CFD simulation where it has been evaluated at a plane downstream the blade at 11 points over the radius.

It was then used in TURBOdesign1 and changed iteratively together with the streamwise loading until the blade shape matched the original one. Mri represents the meridional section of the fan, arrow shows main flow direction. Figure 3 shows the outcome of this process. The results in Figure 3 shows that the baseline design has a parabolic spanwise work (or $r\bar{V}_\theta^*$) distribution.

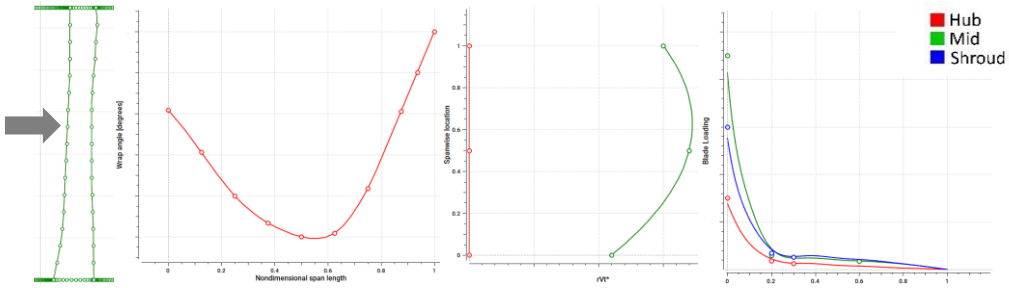

Figure 3: Geometric characteristics of the original fan (from L to R: mri, spanwise load, streamwise load, wrap angle)

The streamwise loading is fore-loaded at the hub (section 1), midspan (section 2) and Shroud (section 3). The streamwise loading shows high leading edge loading ($\partial\left(r\overline{V_\theta}\right)/\partial m$) at all sections from hub to tip indicating a design with relatively high AoA or incidence. The AoA or incidence is set by the leading edge value of streamwise loading (or $\partial\left(r\overline{V_\theta}\right)/\partial m$). Results shows higher incidence at the midspan. Also the last plot in Figure 3 shows the variation wrap angle at the stacking condition on the baseline design. This type of stacking condition normally results in a forward swept geometry for the fan and indeed the baseline fan has a forward swept geometry.

CFD SIMULATION

Setup

Numerical simulations were performed on high performance computers (HPC) with ANSYS CFX v 19.2. 10 steady-state simulations were carried out for the reference fan for and each of the new designs for flow rates from 10 to 100 %, where 100% is the maximum flow-rate at 0 pressure difference. The SST turbulence model of Menter [14] was chosen for the CFD simulations because it shown very good predicting capability by Bardina *et al.* [15], Hirsch [18] as well as Bleiziffer in [6], [11] and [14]. The automatic adaptive wall functions implemented for the near-wall treatment of turbulence in ANSYS-CFX were used in the simulations. The rules about the correct grid treatment for computations of internal flows using two-component turbulence models from Peric [17] and Hirsch [18] as well as in the CFX-Solver Manual [16] were followed while generating the meshes. In the mentioned works the most accurate grid for practical use is a structured grid, which was used for the fan domain in this study. For the present case fan domain meshes having both smaller (half) and larger element size (double) did not show a significant change of the solution (within ± 2 %, Figure 4).

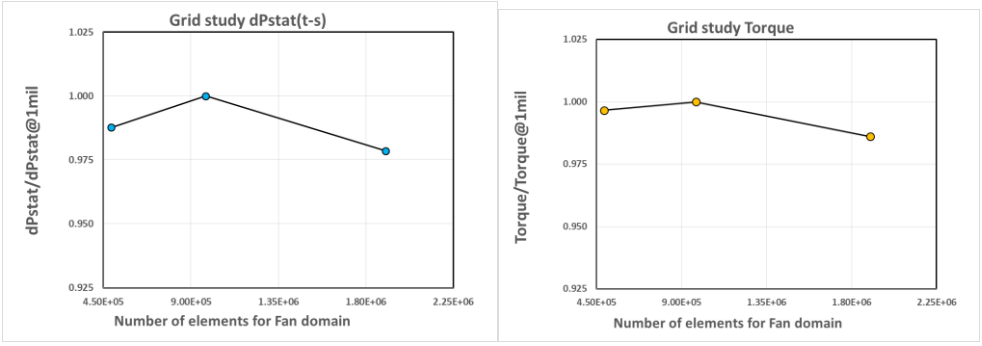

Figure 4: Grid study for the fan domain

The CFD model was divided in 3 computational domains: the inlet domain, the fan domain (rotating) and the outlet domain. Inlet and outlet domain also incorporate the flow domain (tip strip) between fan-ring and the shroud (see details in Figure 5b). For avoiding inconsistencies in the numerical computation due to large unsteady effects behind the impeller, outlet domain was generated much longer and wider (>10 fan diameters). Blades and their corresponding structured meshes were generated using Ansys TurboGrid while a single blade of the fan is used for the CFD

simulations by using periodical boundary conditions. Axis symmetrical slices of inlet and outlet domains were generated using Ansys Design Modeler including the above mentions tip strip. An unstructured mesh including near wall refinement (8 prism layers) was generated for these domains with particular attention to the interfaces (Figure 5b). For the rotor-chamber-interface and the rotor-outlet-interface a stage interface was used by specifying the correct pitches. The gap between fan ring and shroud is modeled as a channel in the inlet and outlet domains and are connected via a GGI interface. Simulations are performed automatically starting with a zero total pressure boundary condition at the inlet surface and all other points on the fan curve using a mass flow boundary condition as a percentage of the maximum flow. The outlet boundary condition was specified as an opening at the atmospheric pressure. A constant rotational speed was applied to the rotating domain. The ambient temperature was set at 25°C. The flow-rate and pressure at the interfaces as well as at the inlet and outlet were monitored in the solver during the simulation. Solution was stopped either after reaching a maximum number of iterations or after the statistical convergence of monitor points was achieved (pressure and torque). Green points in Figure 6 converged after the statistical convergence was achieved, yellow had a fluctuation around mean value (of last 25 iterations) lower than ±1.5 %, red between ± 1.5 % and ± 2.5 %, and were stopped after 300 iterations.

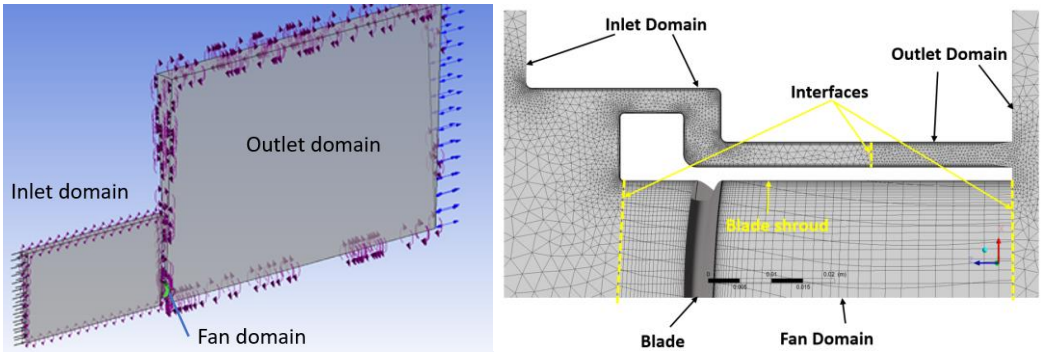

Figure 5: a) complete CFD Setup b) mesh details at the blade tip (section in axial direction)

Correlation to test-rig and mesh accuracy

While enhancing the current CFD design process, a correlation between test-rig results and CFD results has been established. Parameters of both simulation and experiment have been adjusted in order to correlate results of the CFD simulation with measurements. The mesh used was the middle size in Figure 4 (~1mil elements for the fan domain).

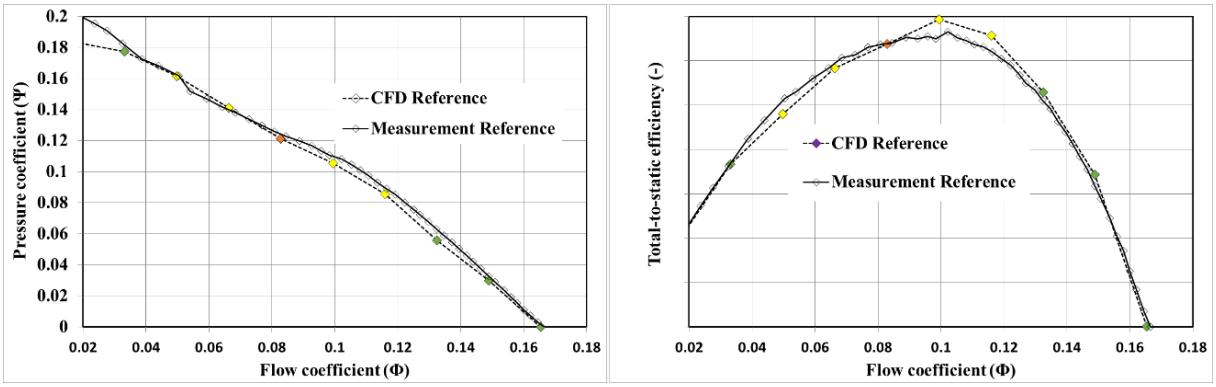

Figure 6: Comparison between measurement and CFD simulation for a reference fan

The test has been performed using an aluminum milled fan sample (of a serial fan) which was powered by an external drive. The measurement has been performed at the same constant speed as in the simulation. Results are shown in Figure 6. Both pressure and efficiency are very well predicted by CFD. As a consequence the mesh and setup were used as a baseline for the new development.

EXPERIMENTAL SETUP

ISO 5801 Performance test rig & semi-anechoic acoustic chamber

Hanon Systems uses a certified ISO 5801 (figure 7a) test rig for measuring fan performance. Data acquisition is completely automated and fans can be driven either by their own electric drive or they can be driven by an external electric drive (up to 3kW power). For the external drive measurement a torquemeter is used to measure the torque. The measurement with external drive is standard for all new developments. NVH measurements have been performed in a semi-anechoic room of Hanon Systems in Kerpen, Germany. Fans were suspended on an aluminum frame as shown in Figure 5b and 2 Brüel & Kjær 4189 -A-021 1/2" free-field microphones are placed in front of it. One is placed 1m in horizontal direction in front of the fan hub while the other is placed 30° on the side of the fan (Figure 7a). Measurements are performed during ramp-up and -down to the highest rpm of the fan.

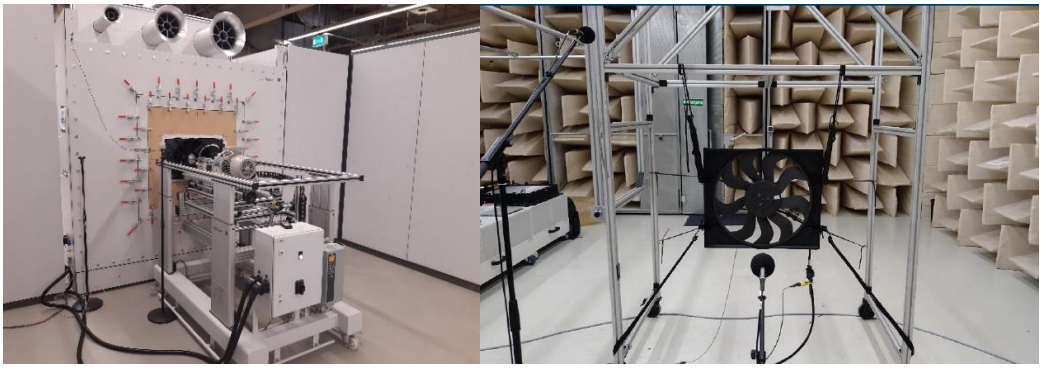

Figure 7: a) ISO 5801 Airflow test stand with external drive at Hanon Systems in Bad Homburg (serial sample is shown) b) Semi-anechoic room with sample fan and two microphones (Hanon Systems, Kerpen, Germany)

RESULTS AND DISCUSSIONS

Aerodynamic performance

The spanwise work or (or $r\bar{V}_\theta^*$) distribution specified in the 3D inverse design method is related to the total-total (t-t) or to the total-to-static (t-s) pressure over the fan stage, through the Euler equations. As mentioned in the introduction, several publications [6,9] show that the correct performance parameter for axial fans design is the total-to-static rig pressure as this is the performance measured on an ISO 5801 test rig (Figure 8).

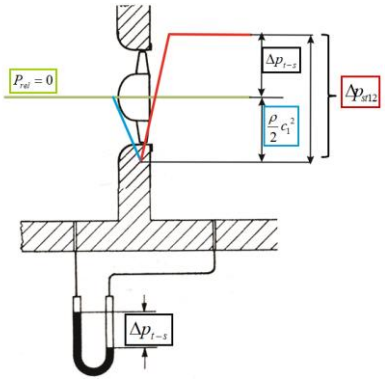

Figure 8: Explanation of the total-to-static rig pressure for an axial fan stage (Bleiziffer [6])

This quantity differs from the static-to-static or total-to-static pressure of an axial fan stage section as shown by Bleiziffer [6]:

$$\Delta p_{t-s} = \Delta p_{st12} - \frac{\rho}{2}c_2^2 \tag{3}$$

$$\Delta p_{t-s} = (U^2 - c_1^2(\tan(\beta_2))^2) - \frac{\rho}{2}c_2^2 \tag{4}$$

As a consequence a total-to-static ideal rig efficiency can be derived for a section as [6]:

$$\eta_{t-s} = \frac{\Delta p_{t-s} \cdot Q}{\Delta p_{t-t} \cdot Q} = \frac{\Delta p_{t-s}}{\Delta p_{t-t}} \quad (5)$$

The above equations were integrated radially for a specific spanwise load distribution (for free vortex Bleiziffer [6]) and for non-free-vortex and considering radial balance equations Semel [8,10].

Meridional section (mri) of the re-engineered design has been scaled and adjusted to the new dimensions as shown in the picture bellow. Thickness was adapted after the structure stresses and frequency of the final design have been calculated and they reached the internal specifications in terms of durability.

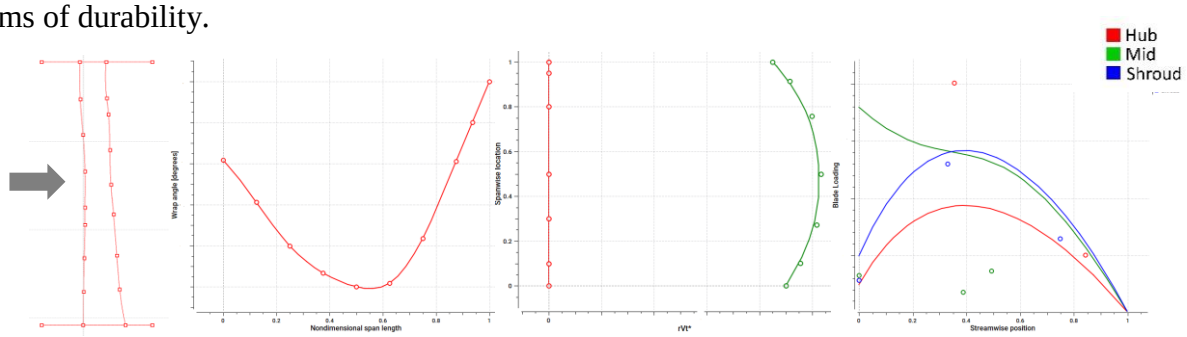

Figure 9: Geometric characteristics of the final fan (from L to R: mri, wrap angle, spanwise and meridional load)

The wrap angle used at stacking condition in the design is similar to that distribution of the baseline design. The load distribution has been varied iteratively so that the desired pressure has been reached at the design flow-rate. The final parameters of the design can be seen in Figure 9. The spanwise work (or $r\bar{V}_\theta^*$) shown in Figure 9 has the same parabolic distribution from Hub to shroud as the baseline case shown in Figure 3. The streamwise loading is also fore-loading but with only high values of leading edge loading or $(\partial(r\overline{V_\theta})/\partial m)$ at the midspan. Indicating that this design has a bit higher incidence or (AoA) at midspan but then generally lower incidence at hub and tip sections. After performing structural analysis of the resulting blade in order to ensure its structural integrity, the final design has been prototyped. The fan prototype is shown in Figure 11 b. The fan has been milled out of aluminum and has been tested on the test rig using an external drive and an adaption ring instead of the shroud. This was attached to the shaft of the external drive and has been driven at the constant rpm value used in the design. A comparison between measurement and CFD simulation of the new fan is shown in Figure 10.

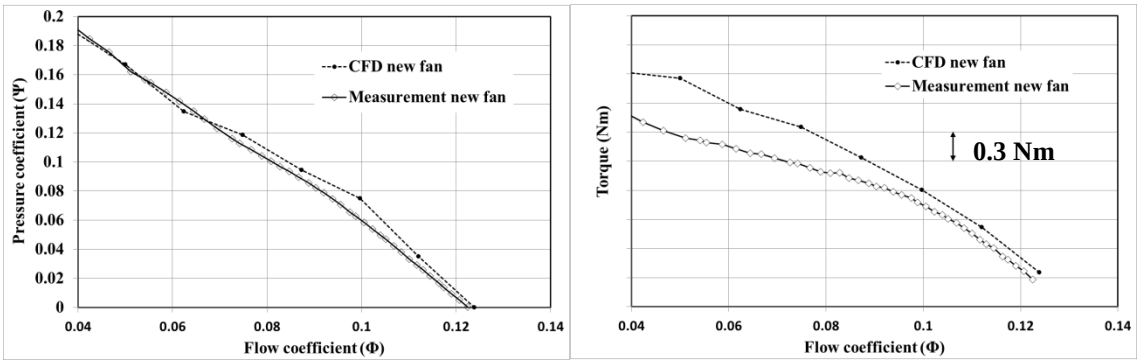

Figure 10: Measured and simulated pressure and torque

Pressure is well predicted everywhere on the fan's curve while the torque is well predicted on flow regions above 60 % of the maximum flow ($\Phi > 0.08$). While prediction at high flow rates does not represent a problem, the prediction below 60 % is difficult for turbomachines when using steady-state simulations as the flow usually separates and the solver cannot capture the unsteady flow in a steady simulation. The maximum flow-rate is very well predicted while torque is over predicted at flow-rates below 60 % ($\Phi < 0.08$). See also the details in the CFD Simulation section regarding convergence.

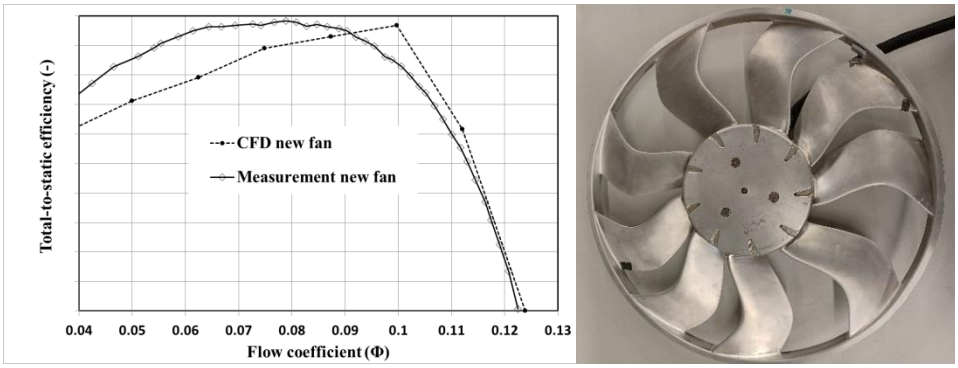

Figure 11: a) Measured and simulated efficiency b) New fan as milled aluminum prototype

Efficiency curves comparison shows a good prediction above 70 % flow-rate. Its peak is the same as in the simulation but is reached at a lower flow-rate as predicted by the CFD (Φ 0.08 instead of 0.1). Below 60 % flow-rate (Φ < 0.08) the difference in the efficiency reaches in some point 5-6 % but this region is outside the working range of the designed fan.

NVH performance

NVH measurements were performed on both fans according to the specifications shown above for their complete rpm range using only the horizontal front microphone. In order to better compare them a relevant speed range of the fans was chosen, while also normalizing it by the tip diameter (to tip speed). The new fan was 3D printed (SLS from PA-CA material) at a scale of 97 % of the original tip diameter for acoustic measurements since this was required by a new application. The reference fan (serial) was finished out of plastics (PA6-GF30). Distance between fans and struts were similar. The results of the ramp-up measurements are shown in Figure 12. Above a tips speed of 27 m/s the new development shows an improvement of the SPL between 3 and 5 dB(A) in the relevant working range.

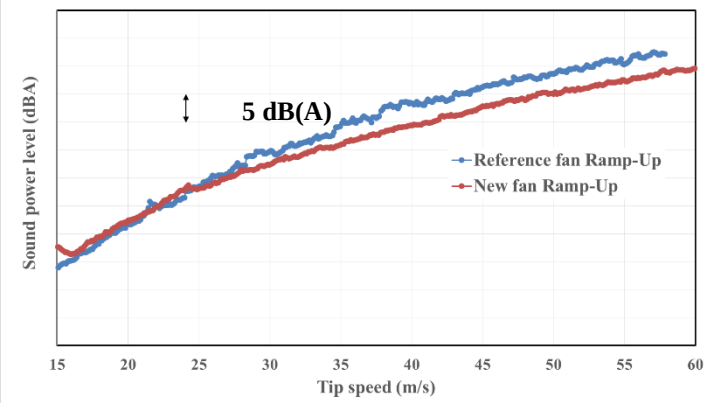

Figure 12: Measured sound pressure level of both fans shown in the relevant working range

CONCLUSIONS

This study has shown how efficient design features available in legacy designs can be integrated in new designs by using 3D inverse design method and the reverse engineering functionality available in commercial 3D inverse design code TURBOdesign1. The reverse engineering process helps to capture the main know-how in the design of previous optimum fans in terms of main inputs of inverse design method such as spanwise work, streamwise loading and stacking conditions. Starting from these previous optimum input specifications the inverse design method can be quickly used to optimize fans with new specifications in terms of diameter, flow rate, pressure rise or torque. It is also shown that the new fan design shows improved efficiency and improved acoustic.

ACKNOWLEDGEMENTS

Special thanks have to be made to Lorenzo Bossi from the London office of ADT. The support of Erhan Dinc and Christian Schmitt for providing the design and mechanical simulation in Bad Homburg Office and of Philipp Benjack, Philip Gallisch and Balthasar Schillemeit from Kerpen Office for providing us the acoustic measurement data is gratefully acknowledged. The authors also thank the company Hanon Systems for agreeing to publish the data in this paper.

BIBLIOGRAPHY

[1] M. Zangeneh – *A compressible three-dimensional design method for radial and mixed flow turbomachinery blades* International Journal for Numerical Methods in Fluids, 13 (5) 599 – 624, **1991**

[2] H. Okamoto, M. Zangeneh, H. Watanabe, A. Goto – *Design of a box fan rotor using 3-D inverse design method* IMechE International Conference on fans, 9-10 November 2004, London, **2004**

[3] M. Henner, Y. Beddadi, B. Demory, M. Zangeneh and F. Pengue – *Automotive blower design with inverse method applied on wheel and volute* Proceedings of Fan2015, International conference on Fan Noise, Technology and Numerical Methods, Lyon, **2015**

[4] H. Okamoto, A. Goto, M. Furukawa – *Design Of A Propeller Fan Using 3-D Inverse Design Method And CFD For High Efficiency And Low Aerodynamic Noise* ASME paper FEDSM2009-78454, **2009**

[5] L. Zhang, G. Davila, and M. Zangeneh – *Multi-objective optimization of a high specific speed centrifugal volute pump using three dimensional inverse design coupled with computational fluids dynamics simulation* Journal of Fluids Engineering, 143(2):021202, Feb. **2021**

[6] M. Miclea-Bleiziffer, P. Epple, H. Smith, M. Semel, A. Delgado – *Application of an Inverse Cascade Analytical and Numerical Design Method Used in the Design of Axial Fan* Proceedings of the ASME Turbo 2011, GT2011-45860, pp. 457-470, **2011**

[7] H. Smith, M. Semel, P. Epple, M. Miclea-Bleiziffer, A. Delgado – *Accurate Calculation of the Slip Factor of Axial Cascades and Impellers for Arbitrary Blade Shapes* Proceedings of the ASME Turbo 2011, GT2011-46352, pp. 523-537, **2011**

[8] M. Semel, P. Epple, M. Miclea-Bleiziffer, A. Delgado, H. Smith – *Extended Mean Line Theory for Axial Fans: Analytic Calculation of the Flow Characteristics for Off-Design Points* Proceedings of the ASME Turbo 2011, GT2011-46268, pp. 509-522, **2011**

[9] P. Epple, F. Durst, A. Delgado – *A theoretical derivation of the Cordier diagram for turbomachines* Proc. IMechE Vol.225, issue 2, Part C: J. Mechanical Engineering Science, **2011**

[10] M. Semel – *Der Einfluss der Arbeitsverteilung auf die Kennlinie einstufiger axialer Strömungsmaschinen*, PhD Thesis, FAU Erlangen-Nuremberg, **2019**

[11] M. Bleiziffer, A. Untaroiu, A Delgado – *Development of a novel design method for marine propellers by computing the exact lift of arbitrary hydrofoils in cascades* Ocean Engineering, Volume 83, pages 87-98, **2014**

[12] I.H.A. Abbott, A.E. von Doenhoff – *Theory of wing sections, including a summary of airfoil data* Dover Publications, **1959**

[13] M. Bleiziffer – *Development of an inverse design method for propellers with application on left ventricular devices* PhD Thesis, FAU Erlangen-Nuremberg, **2017**

[14] F.R. Menter – *Zonal two-equation k-ω turbulence models for aerodynamic flows* AIAA paper 96-2906, **1993**

[15] J.E. Bardina, P.G. Huang, T. J. Coakley – *Turbulence Modeling Validation Study* NASA Ames Research Center September, **1998**

[16] ANSYS CFX-Solver Modeling Guide,Release V19.2 Ansys Inc. **2019**

[17] J.H. Ferziger, M. Peric – *Computational Methods for Fluid dynamics* Springer, **2002**

[18] C. Hirsch – *Numerical Computation of Internal and External Flows* Volume 1: Fundamentals of Computational Fluid Dynamics, Second edition, Elsevier **2007**

[19] TURBOdesign Suite 2021R1 – Advanced Design Technology Ltd, **2021.**